



Prediction of synthetic oil parameters by artificial neural networks at durability tests of porous bearings

Artur Król^{a*} and Krzysztof Gocman^b

^a Military University of Technology, Faculty of Logistics, 2 Gen. Kaliskiego St., 00-908 Warsaw, Poland

^b Military University of Technology, Faculty of Mechanical Engineering, 2 Gen. Kaliskiego St., 00-908 Warsaw, Poland

Received 9 September 2015, revised 8 December 2015, accepted 9 December 2015, available online 7 March 2016

Abstract. In this article we use artificial neural networks (ANN) in durability analysis of porous bearings. First, we present briefly the results of durability tests of porous sleeves impregnated with synthetic ester oil under different duration of the tests (100, 500, and 1000 h) and bearing temperature (60, 80, and 130 °C) at a rotational speed of 1000 rpm. After each durability test oil samples were removed from the bearings and some chosen parameters were checked (Fourier Transform Infrared spectra and total acid number). In the second stage, the collected data were used in the design of ANN, i.e. work parameters as the inputs and oil properties as the outputs. The tests of various ANN types were performed to achieve the smallest training error and the best performance. The best parameters were achieved for multilayer perceptrons neural networks, and also quite good prediction of oil parameters after the test was observed. The achieved results, i.e. the ANN designed, algorithms, and oil parameters used, were compared with those observed in the previous tests for mineral oil.

Key words: porous bearings durability, oil ageing, artificial neural networks.

1. INTRODUCTION

1.1. Porous bearings characteristics

One of the various types of conventional sliding bearings is porous bearing, having its structure filled with oil. The lubricant should be chosen carefully, regarding work conditions, as the properties of the lubricant can affect the main features of the bearing – self-lubricating ability and durability [1,2]. The crucial parameters of oil influencing the characteristics of porous bearings are its volatility, oxidation resistance, and lubricating properties [2,3].

Tests of porous bearings lifetime have been conducted rather seldom because this is an expensive and time-consuming study. However the published results show that the oxidation of oil was much deeper [3,4] after work under boundary conditions and essential lubricant additives could be damaged, as revealed by the tests of the Fourier Transform Infrared (FTIR) spectrum [5].

Moreover, the prediction models of porous bearings durability [6] and oil state after durability tests have been presented [7].

1.2. Artificial neural networks

Artificial neural networks (ANN) are believed to be a useful and flexible mathematic tool [6–9]. An interest in ANN use in data analysis is growing and a great number of ANN-implemented models are observed in various disciplines, e.g. medicine, finance, mechanics, tribology, and logistics [9]. The popularity of ANN use derives from their special features [8,10] such as the ability to approximate nonlinear functions, fast and effective multi-processing of large amounts of data, and the ability to learn and adjust a final model to given real data.

The human biological neuron is the foundation of ANN structure and main terms. It receives an electrical or chemical signal by synapsis of dendrites and transfers it through the soma (main body) and axon, by synapsis to the subsequent neurons. As a consequence, the mathematical model of a single neuron is presented as a

* Corresponding author, artur.krol@wat.edu.pl

single nonlinear and parametrized function, according to the following formula:

$$y = f(x_1, x_2, \dots, x_n; w_1, w_2, \dots, w_k), \quad (1)$$

where x_1, x_2, \dots, x_n represent variables (inputs), w_1, w_2, \dots, w_k are parameters (connections or weights), and $f(x; w)$ is the activation function, setting the output (y) of the neuron to the appropriate ranges. However, the structure of ANN could be more complex with the input layer, collecting signals and entering them to the network, the hidden layer, with neurons transforming data and the output layer of neurons working out the output signals.

There are various types of ANN architecture [10]:

- feedforward networks (static), e.g. multilayer perceptrons (MLP) networks,
- feedback or recurrent (dynamic) networks, e.g. Hopfield networks,
- competitive learning networks, e.g. Self Organizing Feature Map (SOFM or Kohonen).

The feedforward MLP networks are useful in the analysis of technical systems, e.g. mechanics, electronics, informatics, and also in various aspects of tribology, especially in fault detection and diagnosis in machinery [11]. A number of learning rules are available, but the main algorithm of the learning process of MLP is the back-propagation method (BP) [10–12]. The method involves the calculation of connection weights and the determining of connection patterns. Signals from the inputs through the hidden layer reach the outputs, and then are again transferred back to the inputs for learning. The non-linear relationship among the inputs and the outputs is estimated by adjusting the weight values and finally it is generalized for the inputs, not comprised in the training data. The BP algorithm searches for a minimum of the error function adjusting the weights by the method of gradient descent [12].

1.3. Application of ANN in tribology

The authors of [13] first showed that ANN could be used in the detection of rolling bearing faults and even ANN of small structure could be a worthy mechanism for fault recognition. An extensive summary of the ANN applications in bearing fault diagnosis in machines is presented in [14]. It clearly explains the rules of appropriate selection of inputs and outputs for the ANN design and the method for bearing life prediction.

The use of ANN in the analysis of lubricants parameters is presented in [12,15,16], but they have been used rather seldom in useful life prediction analysis [15]. The authors of [12] put forward the idea of transformers oil prediction with ANN and conclude that even a lack of sufficient data to train the network results in acceptable accuracy levels. The ANN are also applied in the prediction of fuels parameters [16] using near-infrared spectroscopy.

1.4. Summary of literature review and aim of the research

The suitability of ANN application in the analysis of bearings characteristics and assessment of lubricant properties has been confirmed and presented by various authors. However, only few articles focus on the durability of porous bearings and lubricants used.

The first attempt to use ANN for the estimation of mineral oil state after durability tests was presented in [7]. It was reported that the oxidation process of mineral gear oil could be predicted with MLP neural networks.

However, the oxidation process of mineral oil was much deeper than for synthetic ester oil having better oxidation resistance. Therefore, in that stage it was assumed that ANN prediction of the chosen parameters of synthetic oil with higher oxidation resistance would be possible with acceptable performance and fault parameters. The main aim of the present article was to design ANN for synthetic oil parameters after the oxidation process during porous bearing durability tests.

2. EXPERIMENTAL DETAILS

Experimental details of the test stands were presented in papers [3,4,7], fully describing the main tester of the porous bearing durability and the additional equipment used for oil properties research. The views of the research module and the tester are presented in Figs 1 and 2.

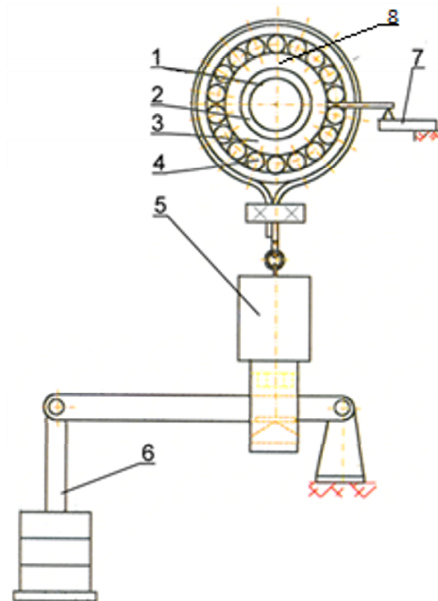


Fig. 1. View of the research module: 1, steel shaft; 2, porous sliding bearing; 3, bearing mounting; 4, needle bearing; 5, load sensor; 6, arm with weights; 7, sensor of friction force; 8, thermocouple.

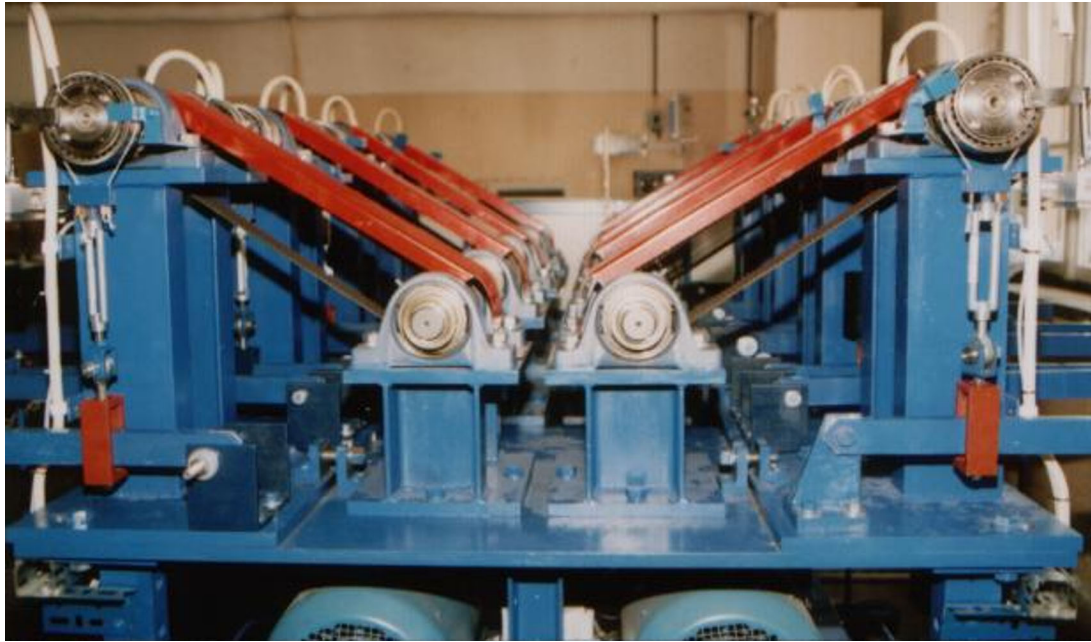


Fig. 2. General view of the durability tester of porous sliding bearings.

The research programme was divided into two main stages: experimental tests and ANN analysis. The experimental tests were completed for the following objects: the porous sliding bearings (Fe powder 97.5%, Cu powder 2.5%) having open porosity 21.5%, and the bush size was $25^{-0.1}/35.2^{-0.16} \times 20^{-0.3}$ mm; the NC6 steel shaft, having 60 HRC hardness; and two oils – mineral gear oil (results of ANN analysis presented in [7]) and synthetic gear oil.

First, the basic properties of fresh synthetic and mineral gear oil (density, dynamic viscosity, lubricity parameter Go_{Z150} , total acid number TAN, Noack evaporation loss Δm), presented in Table 1, were tested according to the standardized methods [16–21].

Then the tribological tests were executed, with continuous measurement of the moment of friction and bearing temperature, i.e. 1000, 500, and 100 h durability tests at 1000 rpm, under the chosen load and three stable

controlled temperatures (60 °C and 1.12 MPa, 80 °C and 130 °C under 1.45 MPa). The housing of the bearing was equipped with the electric heating module to control and stabilize (± 5 °C) the temperature during the tests. The 1000 h test at stable 80 °C was prolonged to 4008 h, as after the 500 h test no significant changes in lubricant properties were observed. Additionally, as the temperature of 80 °C is believed to be a typical boundary temperature of porous bearing filled with lubricant, it was reasonable to enhance the tests.

After the tests the oil samples were extracted and collected for the testing of TAN and FTIR spectroscopy analysis. The FTIR method is widely used [5,15,16,22] in observing the oxidation process of oils, i.e. chemical changes in the lubricant base and comprised functional additives. The tests were realized with Nicolet iS10 spectrometer by Thermo Scientific having the IR source, DTGS KBr detector, and KBr beamsplitter

Table 1. Basic parameters of fresh mineral gear oil [7] and synthetic ester oil

Oil	Density, g/cm ³		Dynamic viscosity, mPa·s		Lubricity parameter Go_{Z150} , MPa	Total acid number, mgKOH/g	Noack loss Δm , %
	40 °C	100 °C	40 °C	100 °C			
Mineral	0.880	0.853	171.8	15.30	38.3	1.01	6.5
Synthetic	0.848	0.838	96.8	12.77	7.8	2.15	15.9

(4000–650 cm^{-1} , 32 scans, 4 cm^{-1} resolution, Happ–Genzel apodization). The sampling FTIR technique was attenuated total reflection, as it is a fast, easy sample preparation technique (no dilution required), and radiation is not transmitted through the sample [23]. As previously in [7], the FTIR analysis was based on American Society for Testing and Materials (ASTM) standards [23,24], covering practices for monitoring the conditions of in-service lubricants.

The ANN analysis was performed in the second stage with Statistica Neural Networks comprising the design of ANN, learning process, and testing process. The data vector was based on the data from the tribological tests (23 cases) and regression MLP were created with different activation functions (sigmoid, hyperbolic, exponential, etc.). The crucial matter at this stage was to decide about the input and the target variables (outputs). As the output parameters should depend on the inputs, the inputs were work conditions, i.e. p – pressure from the bearing load, v – sliding velocity, T – work temperature, t – duration of the test, and the outputs were the oil parameters studied after the tests (TAN and selected peaks of FTIR spectra).

The learning process with different iterative techniques was to adjust the weights of ANN to produce an output which is as close as possible to y for any given input data x . The performance of ANN was estimated during the testing process (prediction for unseen data), which is known as generalization. Therefore the collected data were divided for use in the learning (80%) and testing process (20%). The process of ANN creation consisted of the following steps:

- presenting to ANN each input–target pair from the training data,
- calculation of the outputs – predictions of ANN for the targets,
- calculation of the error function – (Eq. 2),
- for better predictions for each input–target pair, the adjustment of the ANN weights with the training algorithm,
- use of separate testing data to compute predictions and the value of the test error,
- checking the test error value: if decreasing, continue training, if otherwise, stop training,
- estimation of the training performance P_{tr} and the testing performance P_t for the designed ANN.

The error function, the difference between the output and target values, was calculated according to the following formula:

$$E = \sum_{i=1}^n (y_i - a_i)^2, \quad (2)$$

where y_i is the calculated output of the ANN, a_i is the target (aim – real value) of the output, i is the number of the consequent case, n is the total number of cases.

3. RESULTS AND DISCUSSION

3.1. Tribological tests

The tribological characteristics were quite stable at smaller temperatures, i.e. at 60 and 80°C. The example of the single test presented in Fig. 3, for study at constant temperature of 130°C, shows that the tests at the increased temperature were not finished because of a bearing seizure.

After initial stable work, the moment of friction and temperature increased rapidly, indicating the seizure process (Fig. 3). Thus the 130°C temperature was unacceptable work condition compared to 60 and 80°C and mass loss of oil was very intensive. The probable reason was much higher volatility of synthetic oil compared to mineral one (Table 1) used in previous tests in [7].

After the tests, the TAN of oil samples was checked. Small fluctuations were observed for temperature and test duration increase (the values 1.85–3.89 mgKOH/g at 60 and 80°C and 1.45–2.56 mgKOH/g at 130°C). However, it was clearly seen the TAN did not reach the values observed for mineral oil (1.29–4.02 mgKOH/g at 60 and 80°C and even 27.07 mgKOH/g at 130°C [7]).

The oxidation process of oil was defined during the analysis of FTIR comparative spectra for different work conditions (Fig. 4).

Significant dissimilarities of oil spectra occurred at 80 and 130°C and at prolonged duration of the tests. The differences were observed for peaks of oxidation resistance additive (1594 and 1530 cm^{-1}) within the oxidation range (1800–1670 cm^{-1}) and lubricity additive (1164 and 960 cm^{-1}). Work at a higher temperature was the main reason for deeper oxidation and resulted in the creation of acid carbonyl structure peaks (1710 and 1770 cm^{-1}) at a strong ester peak (1740 cm^{-1}). The selected peaks area and TAN value were consequently used as the outputs in ANN creation.

3.2. Design of artificial neural networks

As mentioned above, ANN had strictly specified inputs, as a consequence of performed tribological tests (work parameters), i.e. p , v , T , and t . The outputs of ANN were parameters of oil investigated after the tests, i.e. the TAN value, S_{AW} antiwear additive peak area (960 cm^{-1}), S_{OP} oxidation products peak area (1800–1670 cm^{-1}), and S_{EP} area of ester peaks (1760–1720 cm^{-1}). Finally, each ANN had three inputs and one target.

Tables 2 and 3 present examples of calculations of ANN, having the best training performance P_{tr} , and test performance P_t (as close as possible to 1) and the smallest training and test error (E_{tr} , E_t). The results of sensitivity analysis parameters, estimating the importance

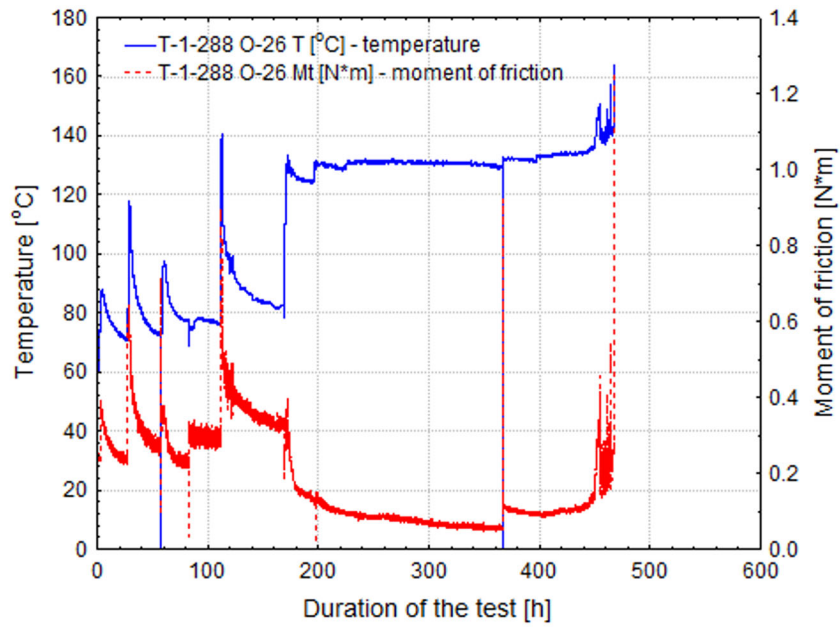


Fig. 3. The single durability test of the bearing No. 288 ($T = \text{const} = 130^\circ\text{C}$, duration 500 h) – moment of friction and temperature of the bearing.

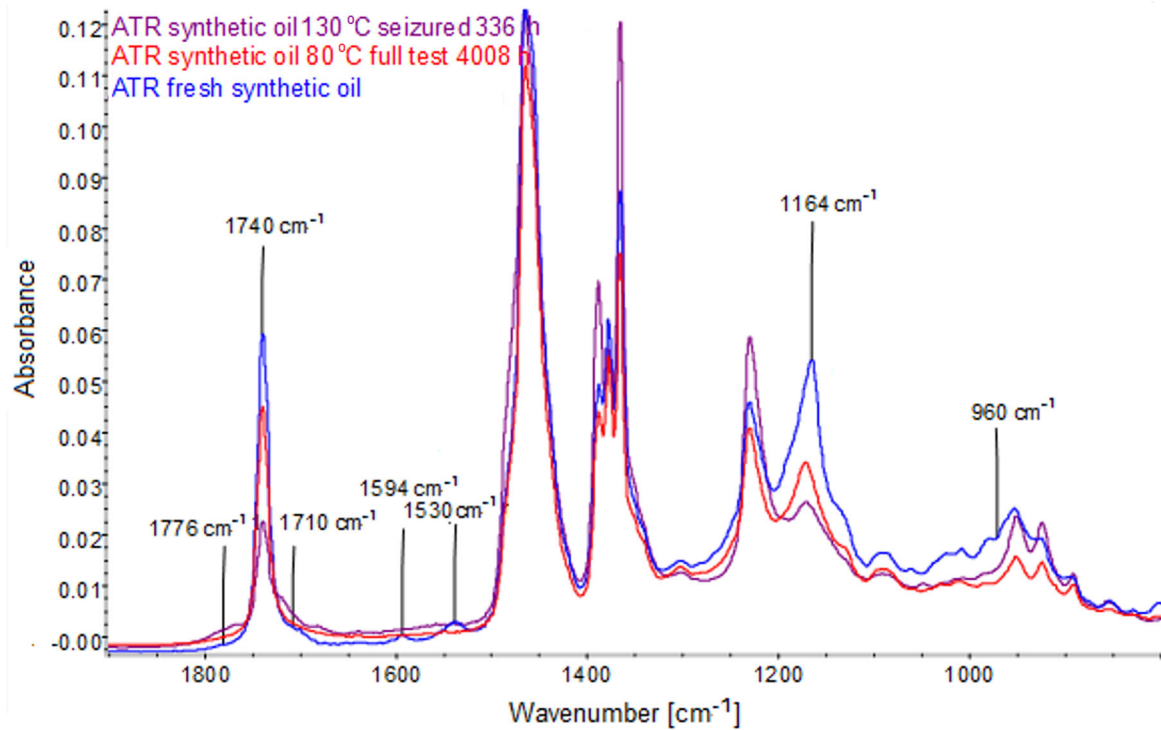


Fig. 4. Comparison of fresh synthetic oils and oils from bearings after the test at 80°C (4008 h) and 130°C (500 h test – seizure after 336 h). ATR, attenuated total reflection.

Table 2. Results of the calculation of artificial neural networks (ANN) with pressure (p), duration of the test (t), and temperature (T) as inputs and the total acid number (TAN) and oxidation products peak area (S_{OP}) as outputs. P_{tr} , training performance; P_t , test performance; E_{tr} , training error; E_t , test error; AF, activation function

Output – TAN					
ANN	P_{tr}	P_t	E_{tr}	E_t	AF
3-2-1	0.952	0.926	0.004	0.007	Tanh
	Sensitivity analysis of ANN inputs				
	p	t	T		
	2.09	11.38	1.84		
Output – S_{OP}					
ANN	P_{tr}	P_t	E_{tr}	E_t	AF
3-1-1	0.888	0.992	0.012	0.001	Logistic
	Sensitivity analysis of ANN inputs				
	p	t	T		
	3.67	1.54	5.10		

Table 3. Results of the calculation of artificial neural networks (ANN) with pressure (p), duration of the test (t), and temperature (T) as inputs and antiwear additive peak area (S_{AW}) and area of ester peaks (S_{EP}) as outputs. P_{tr} , training performance; P_t , test performance; E_{tr} , training error; E_t , test error; AF, activation function

Output – S_{AW}					
ANN	P_{tr}	P_t	E_{tr}	E_t	AF
3-1-1	0.710	0.999	0.027	0.002	Tanh
	Sensitivity analysis of ANN inputs				
	p	t	T		
	1.26	1.71	1.08		
Output – S_{EP}					
ANN	P_{tr}	P_t	E_{tr}	E_t	AF
3-3-1	0.917	0.992	0.008	0.001	Identity
	Sensitivity analysis of ANN inputs				
	p	t	T		
	2.90	1.54	11.36		

of the models' input variables, are also presented and output activation functions AF are listed.

Generally, the achieved ANN had high training performance P_{tr} and testing performance P_t , meaning good adjustment of the designed ANN to real data. Training and testing errors had also small values for all presented ANN with specified outputs.

The results of sensitivity analysis (Tables 2 and 3) showed differed impact of inputs on the specified output.

The TAN value was under the strongest influence of time ($t - 11.38$), compared to load pressure ($p - 2.09$),

and temperature ($T - 1.84$). The destruction of antiwear additive was rather under the same comparable influence of all inputs. However, the oxidation products area S_{OP} was visible at a higher impact of temperature ($T - 5.10$) and a similar tendency was observed for ester products area S_{EP} ($T - 11.36$). The duration of the test (t) was not meaningful for these two outputs. This is the consequence of the oxidation process pattern, i.e. small changes in the oxidation area and the ester peak area.

The detailed structures of the achieved ANN are presented in Figs 5–8. The figures show all nodes in layers and adjusted weight values and bias (activation threshold value of the neuron).

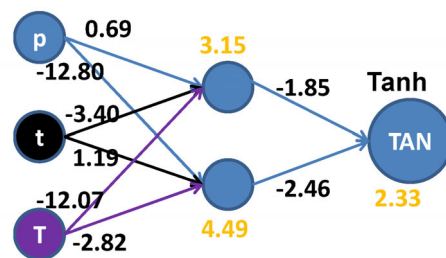


Fig. 5. The structure of 3-2-1 ANN: three inputs (p , t , T) and one output (TAN) with weights (black) and (bias) calculations and the activation function (AF) – Tanh (hyperbolic tangent function).

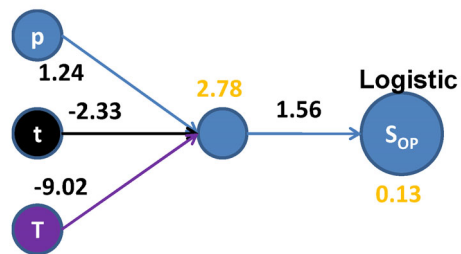


Fig. 6. The structure of 3-1-1 ANN: three inputs (p , t , T) and one output (S_{OP}) with weights (black) and (bias) calculations and activation function (AF) – Logistic (S-shaped sigmoid function).

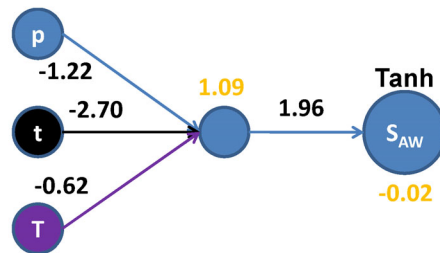


Fig. 7. The structure of 3-1-1 ANN: three inputs (p , t , T) and one output (S_{AW}) with weights (black) and (bias) calculations and activation function (AF) – Tanh (hyperbolic tangent function).

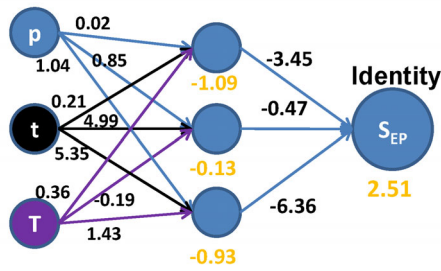


Fig. 8. The structure of 3-3-1 ANN: three inputs (p , t , T) and one output (S_{EP}) with weights (black) and (bias) calculations and activation function (AF) – Identity (input signals are not formed at all).

The presented ANN models had MLP structure, however, with a different number of hidden neurons, weight values, and bias. The structure of the designed ANN was rather simple, giving at the same time high performance and prediction ability.

Finally, the residuals of the designed ANN were analysed. Their values were not always small, meaning that the model was not fully satisfactory. The normality of residuals distribution was evaluated with the Shapiro–Wilk test, a good test for measuring power properties. The test would reveal if the effectiveness of the designed ANN was the same in all the cases.

The full normality analysis of residuals distribution is summarized in Table 4. If the W statistic is significant ($p_{SW} < 0.05$), the hypothesis that the respective distribution is normal should be rejected. This was observed for residuals of ANN with S_{AW} as the output.

The examples of distribution of the residuals are presented in Figs 9 and 10. These show small residual values for TAN as the output (Fig. 9) and higher values for the antiwear additive area S_{AW} (Fig. 10).

The designed ANN were compared with the results for mineral oil [17]. As previously, the best parameters were achieved for MLP neural networks, having also simple structure, i.e. the total number of ANN nodes was rather small. The same ANN structure for both oils was observed for the outputs: TAN (3-2-1), S_{AW} (3-1-1), S_{OP} (3-1-1), but the calculated weights had different values, as a consequence of dissimilar oxidation processes for both oils.

Table 4. Shapiro–Wilk test results for different artificial neural networks (ANN)

ANN structure	ANN output	Shapiro–Wilk parameters
3-2-1	TAN	SW–W = 0.9700; p_{SW} = 0.7556
3-1-1	S_{AW}	SW–W = 0.8501; p_{SW} = 0.0053
3-1-1	S_{OP}	SW–W = 0.9434; p_{SW} = 0.2781
3-3-1	S_{EP}	SW–W = 0.9805; p_{SW} = 0.9401

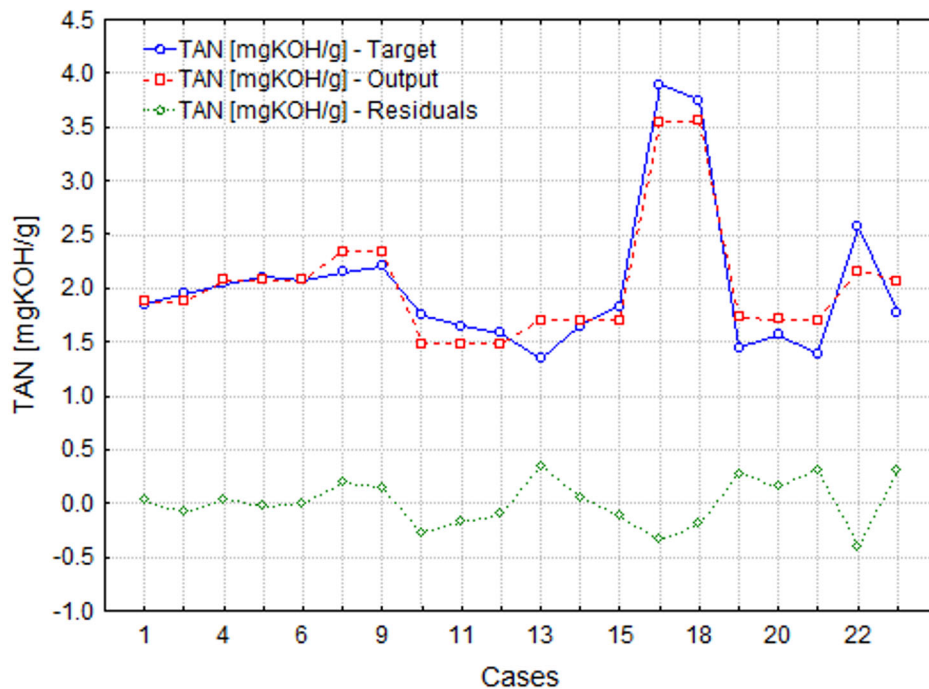


Fig. 9. Comparison of the TAN, TAN output, and residuals of 3-2-1 ANN and for consequent cases.

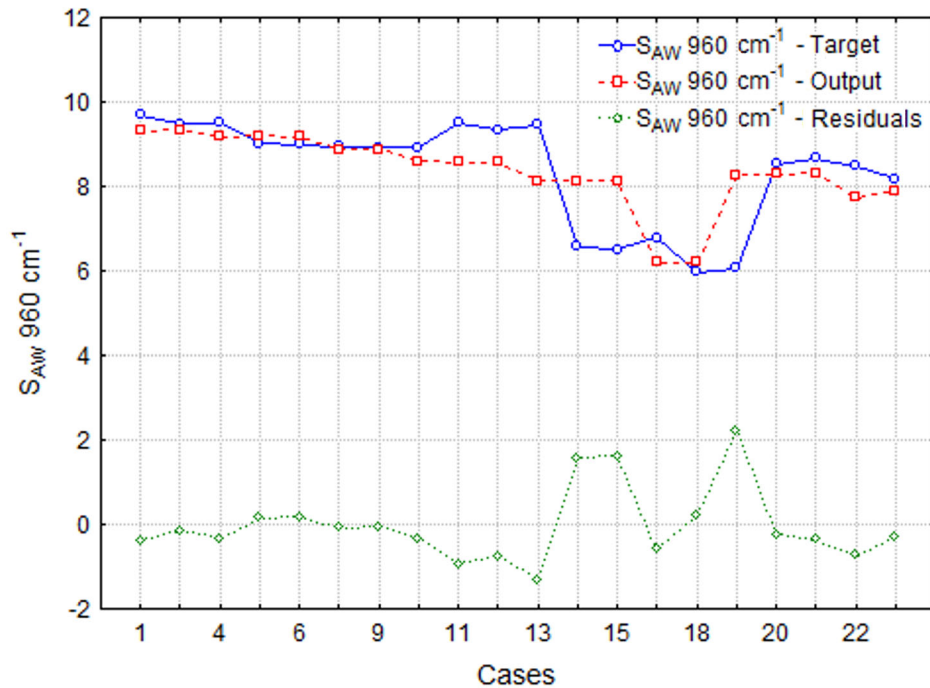


Fig. 10. Comparison of S_{AW} , S_{AW} output, and residuals of 3-1-1 ANN and for consequent cases.

The sensitivity analysis of the inputs showed completely different results, i.e. the TAN as the output was most affected by the duration of the test (t) in the case of synthetic oil, but by temperature (T) in the case of mineral oil [17]. Regarding S_{OP} as the output, the highest influence was exerted by temperature (T) for synthetic oil and also for mineral oil. However, the latter value was smaller compared to the other parameters.

4. CONCLUSIONS

1. Artificial neural networks were designed for synthetic oil parameters after the oxidation process during porous bearing durability tests. The designed ANN had simple structures, but gave high performance, prediction ability, and small faults.
2. It was confirmed that ANN prediction of the chosen parameters of synthetic oil, having better oxidation resistance than mineral oil, was possible with the acceptable performance and fault parameters.
3. Examples of MLP neural networks designed for both mineral and synthetic oils had the same structure (number of neurons in layers), but the sensitivity analysis of input parameters gave different results, as a consequence of the oil oxidation pattern. Moreover, the sensitivity analysis could be used as a good mathematic tool to discover the meaning of work parameters and

their influence on the outputs, especially if the number of inputs is higher.

4. The full normality analysis of residuals distribution of the achieved ANN should be performed to confirm the effectiveness of the network for all cases.

ACKNOWLEDGEMENT

The authors wish to acknowledge the reviewer A. Kulczycki and the anonymous reviewer for their detailed and helpful comments on the manuscript.

REFERENCES

1. Kostornov, A. G. and Fushchich, O. I. Exchange of experience. Sintered antifriction materials. *Powder Metall. Met. C+*, 2007, **46**, 503–512.
2. Miller, H. and Tetzlaff, C. Well Oiled. Special and additional lubricants for sintered metal plain bearings. *Tribojournal – Klüber Lubrication*, 2002, **1**, 6–11.
3. Giemza, B., Kałdoński, T., and Król, A. Problem of the service life of self-lubricated friction couples. *Solid State Phenom.*, 2006, **113**, 399–404.
4. Król, A., Giemza, B., and Kałdoński, T. Study on the oxidation process of mineral gear and PFPE oil during durability tests of porous sliding bearings. In *Proc. STLE/ASME 2010 International Joint Tribology Conference*. 2010, 223–225.

5. Hänel, E., Pahl, W., Haspinger, E., and Schuster, K. D. Optimized tribology in sintered metal plain bearings. Joint research project of GKN and Klüber Lubrication at the Westsächsische Hochschule Zwickau. *Tribology Journal – Klüber Lubrication*, 2007, **2**, 20–23.
6. Gienza, B. *Investigations and Modelling of Operating Characteristics of Porous Sliding Bearings Impregnated by Greases*. Doctoral Thesis, Military University of Technology, Warsaw, Poland, 2007 (in Polish).
7. Król, A., Gocman, K., and Gienza, B. Neural networks as a tool to characterise oil state after porous bearings prolonged tests. *Mater. Sci. – Medžg.*, 2015, **21**, 466–472.
8. Dreyfus, G. *Neural Networks. Methodology and Applications*. Springer, Berlin, Germany, 2005.
9. Król, A. Artificial neural networks and their use in logistics. *Mater. Manage. Logistics*, 2015, **5**, 367–378.
10. *Electronic Statistics Textbook*. Statsoft, 1995 <http://www.statsoft.com/textbook> (accessed 6 Dec. 2015).
11. Ali, Y. H., Abd Rahman, R., and Hamzah, R. I. R. Artificial neural network model for monitoring oil film regime in spur gear based on acoustic emission data. *Shock Vib.*, 2015, **1**, 1–12.
12. Shaban, K., El-Hag, A., and Matveev, A. A cascade of artificial neural networks to predict transformers oil parameters. *IEEE Trans. Dielect. Electr. Insul.*, 2009, **16**, 516–523.
13. Ewert, P. and Kowalski, C. T. Neural detector of rolling bearing faults. *Electr. Machines – Trans. J.*, 2011, **92**, 205–209 (in Polish).
14. Gao, R. X. Neural networks for machine condition monitoring and fault diagnosis. In *Condition Monitoring and Control for Intelligent Manufacturing* (Wang, L. and Gao, R. X., eds). Springer-Verlag, London, Great Britain, 2006, 167–188.
15. Sinha, A. N., Mukherjee, P. S., and De, A. Assessment of useful life of lubricants using artificial neural network. *Ind. Lubr. Tribol.*, 2000, **52**, 105–109.
16. Balabin, R. M., Lomakina, E. I., and Safieva, R. Z. Neural network (ANN) approach to biodiesel analysis: analysis of biodiesel density, kinematic viscosity, methanol and water contents using near infrared (NIR) spectroscopy. *Fuel*, 2011, **90**, 2007–2015.
17. *ASTM D287-12, Standard Test Method for API Gravity of Crude Petroleum and Petroleum Products (Hydrometer Method)*. American Society of Testing and Materials International, West Conshohocken, PA, 2012.
18. *ASTM D445-15, Standard Test Method for Kinematic Viscosity of Transparent and Opaque Liquids (and Calculation of Dynamic Viscosity)*. American Society of Testing and Materials International, West Conshohocken, PA, 2015.
19. *PN-C-04147:1976 Petroleum Products. Test for Lubricating Properties of Oils and Greases (Polish Standard)*. Polish Committee for Standardization, 1976.
20. *ASTM D664, Standard Test Method for Acid Number of Petroleum Products by Potentiometric Titration*. American Society of Testing and Materials International, West Conshohocken, PA, 2011.
21. *ASTM D5800-08, Standard Test Method for Evaporation Loss of Lubricating Oils by the Noack Method*. American Society of Testing and Materials International, West Conshohocken, PA, 2008.
22. Griffiths, R. P. and de Haseth, J. A. *Fourier Transform Infrared Spectrometry. Second Edition*. John Wiley & Sons, New Jersey, USA, 2007.
23. *ASTM E2412-04, Standard Practice for Condition Monitoring of Used Lubricants by Trend Analysis Using Fourier Transform Infrared (FT-IR) Spectrometry*. American Society of Testing and Materials International, West Conshohocken, PA, 2004.
24. *ASTM D7412-09, Standard Test Method for Condition Monitoring of Phosphate Antwear Additives in In-Service Petroleum and Hydrocarbon Based Lubricants by Trend Analysis Using Fourier Transform Infrared (FT-IR) Spectrometry*. American Society of Testing and Materials International, West Conshohocken, PA, 2009.

Sünteesõli parameetrite ennustamine tehisnärvivõrkude abil peale poorsete laagrite kulumiskindluse katseid

Artur Król ja Krzysztof Gocman

On kirjeldatud tehisnärvivõrkude (ANN) kasutamise katset poorsete laagrite kulumiskindluse analüüsil. Esiteks on lühidalt toodud poorsete laagripukside kulumiskatsete tulemused sünteetilise esterõliga erinevatel katseaegadel (100, 500 ja 1000 tundi) ning laagri temperatuuridel (60, 80 ja 130 °C) pöörlemiskiirusel 1000 pööret minutis. Peale iga kulumiskatset eemaldati laagritest õli ja määrati mõningad parameetrid (FTIR-i spekter ning üldhappearv (TAN)). Järgnevas staadiumis kasutati kogutud andmeid ANN-i disainil, s.o tööparameetrid olid sisendiks ja õli omadused väljundiks. Katsetati erinevaid ANN-i tüüpe, saamaks väiksemat hälvet ja parimat vastupanu. Selgus, et parimad näitajad saadi MLP närvivõrkude korral. Peale katset täheldati õli parameetrite küllaltki head ennustatavust. Saadud tulemusi (disainitud ANN), kasutatud algoritme ja õliparameetreid võrreldi varasemates katsetes saavutatutega mineraalõli korral.